Vps34/PIK3C3 deletion in thyroid impairs thyroid hormonogenesis and autophagic flux

Giuseppina Grieco[1], Tongsong Wang[1], Ophélie Delcorte[1], Virginie Janssens[1], Catherine Spourquet[1], Aurélie Strickaert[2], Héloïse P. Gaide Chevronnay[1], Xiao-Hui Liao[3], Benoît Bilanges[4], Samuel Refetoff[3], Bart Vanhaesebroeck[4], Carine Maenhaut[2], Pierre J. Courtoy[1*], and Christophe E. Pierreux[1*#]

[1], Cell Biology Unit, de Duve Institute and Université Catholique de Louvain, 1200 Brussels, Belgium;

[2], Institute of Interdisciplinary Research (IRIBHM); Université Libre de Bruxelles, 1070 Brussels, Belgium

[3], Departments of Medicine (X-H.L., S.R.) and Pediatrics and Genetics (S.R), The University of Chicago, Chicago, Illinois 60637;

[4], UCL Cancer Institute; University College London, 72 Huntley Street, London WC1E 6DD, UK;

[#], correspondence to christophe.pierreux@uclouvain.be

*, equal contributions

Running title : Vps34 controls TH synthesis

Key words : Vps34, thyroid, hormone, organification, autophagy

Dr. Giuseppina Grieco, g.pia@hotmail.it

Dr. Tongsong Wang, tswang0802@hotmail.com

Ms. Ophélie Delcorte, ophelie.delcorte@uclouvain.be

Ms. Virginie Janssens, virginie.janssens@uclouvain.be

Ms. Catherine Spourquet, catherine.spourquet@uclouvain.be

Dr. Aurélie Strickaeart, aurelie.strickaert@ulb.ac.be

Dr. Héloïse Gaide-Chevronnay, heloisegaide@hotmail.com

Dr. Xia Hui Liao, xliao1@uchicago.edu

Dr. Benoit Bilanges, b.bilanges@ucl.ac.uk

Prof. Samuel Refetoff, srefetof@uchicago.edu

Prof. Bart Vanhaesebroeck, bart.vanh@ucl.ac.uk

Prof. Carine Maenhaut, cmaenhau@ulb.ac.be

Prof. Pierre J. Courtoy, pierre.courtoy@uclouvain.be

Prof. Christophe E. Pierreux, christophe.pierreux@uclouvain.be

Abstract (327 words, 350 allowed)

BACKGROUND: The production of thyroid hormones (T_3, T_4) depends on thyroid organization in follicles, lined by a monolayer of thyrocytes with strict apico-basal polarity. Polarization supports vectorial transport of thyroglobulin for storage into, and recapture from, the colloid. It also allows selective addressing of channels, transporters, pumps and enzymes to their appropriate basolateral (NIS and Na^+/K^+-ATPase) or apical membrane domain (pendrin, anoctamin, DUOX2, DUOXA2 and TPO). How these actors of T_3/T_4 synthesis reach their final destination remains poorly understood. Vps34/PIK3C3 is now recognized as a main component in the general control of vesicular trafficking and of cell homeostasis via autophagy. We recently reported that conditional Vps34 inactivation in kidney proximal tubular cells by Pax8-driven excision prevents normal addressing of apical membrane proteins and causes abortive macroautophagy.

METHODS: Vps34 was inactivated using a Pax8-driven Cre recombinase system. The impact of Vps34 inactivation in thyrocytes was analyzed by histological, immunolocalization and mRNA expression profiling. Thyroid hormone synthesis was assayed by ^{125}I injection and by serum plasma analysis.

RESULTS: $Vps34^{cKO}$ mice were born at the expected Mendelian ratio and showed normal growth until postnatal day 14, then stopped growing and died at around 1 month of age. We therefore analyzed thyroid $Vps34^{cKO}$ before postnatal day 14. We found that loss of Vps34 in thyrocytes causes: (i) disorganization of thyroid parenchyma with abnormal thyrocyte and follicular shape and reduced PAS^+ colloidal spaces; (ii) impaired ^{125}I organification at comparable uptake and frequent occurrence of follicles with luminal thyroglobulin but non-detectable T4-bearing thyroglobulin; (iii) severe non-compensated hypothyroidism with

extremely low T_4 levels (<0.25 ± 1.5 μg/dL) and huge TSH plasma levels (19,300 ± 10,500 mU/L); (iv) intense signal in thyrocytes for the lysosomal membrane marker, LAMP-1, as well as thyroglobulin and the autophagy marker, p62, indicating defective proteolysis.

CONCLUSIONS: We conclude that Vps34 is crucial for thyroid hormonogenesis, at least by controlling delivery of apical actors responsible for biogenesis of thyroid hormones on Tg as well as defective proteolytic T_3/T_4 excision in lysosomes.

74 ***Introduction***

75 The main function of the thyroid gland is to produce the hormones, T_3/T_4 and
76 calcitonin, which are essential for the regulation of metabolic processes (1,2). The production
77 of T_3 and T_4 depends on the organization of thyroid epithelial cells, the thyrocytes, into
78 functional and independent units, the follicles. These are composed of a single layer of
79 polarized thyrocytes that form a spherical structure delineating an internal space or lumen
80 where the thyrocyte secretory product, thyroglobulin, is stored in a colloidal form, thus called
81 the colloid lumen. As thyrocytes communicate via gap junctions, each follicle functions as an
82 integrated unit. Thyroid hormone synthesis depends on apico-basal cell polarity that allows
83 localization of channels, transporters, pumps and enzymes at the appropriate membrane
84 domains. Iodide from the bloodstream freely traverses the fenestrated endothelium of the
85 thyroid capillaries and is taken up into thyrocytes via the basolaterally localized Na^+/I^-
86 symporter (NIS), thanks to a Na^+ gradient generated by the Na^+/K^+-ATPase. An alternative
87 basolateral transporter, SLC26A7, has been recently reported to also control iodide uptake,
88 although its role might not be direct (3). Iodide diffuses freely within thyrocytes and is next
89 transported across the apical membrane into the colloid space via apically localized
90 transporters such as pendrin or anoctamin. Iodide is then rapidly oxidized into iodine by
91 thyroperoxidase (TPO) located at the apical membrane, in the presence of H_2O_2, generated by
92 the DUOX2/DUOXA2 apical membrane complex. Iodine is incorporated into accessible
93 tyrosine residues close to N- and C-termini of thyroglobulin (Tg), a large protein secreted by
94 thyrocytes into the colloid space. Iodotyrosine rearranges into hormonogenic peptides, which
95 are the direct T_3 and T_4 precursors. Thyroid hormone synthesis thus requires basal localization
96 of NIS and Na^+/K^+-ATPase, apical localization of pendrin, anoctamin, TPO, DUOX2 and
97 DUOXA2, as well as apical delivery of Tg into the colloid lumen and endocytic uptake of iodoTg

98 into thyrocyte lysosomes (1,2). Specific regulators of thyroid follicular organization have
99 recently been identified (4). Transcriptomic comparison of thyroid FRT cells cultured in 2D
100 monolayers and in 3D spherical follicles indeed revealed involvement of structural and
101 functional cell elements such as adherens and tight junctions (cadherin-16), cytoskeleton
102 proteins, ions channels, proteins involved in differentiation, and components of the trafficking
103 machinery (e.g. myosin-Vb, Rab17)(4).

104 There is strong evidence that vesicular trafficking is critical for apico-basal polarization
105 and epithelial function (5-7), but the role of vesicular trafficking in thyroid function is
106 incompletely understood. Vps34/PIK3C3 (also referred to as type III PI3K) has long been
107 recognized as a main actor involved in the general control of endocytic vesicular trafficking (8-
108 12). Vps34/PIK3C3 also plays an important role in epithelial organization in *Drosophila* (12)
109 and in autophagy (11,14), both in the initiation of autophagosome formation and the
110 progression towards autophagosome-lysosome fusion (15,16). We recently inactivated Vps34
111 in kidney proximal tubular cells (PTC) using Wnt4-Cre and Pax8-Cre (17,18). Wnt4-Cre driven
112 Vps34 excision caused major perinatal lethality, with abnormalities in kidney cortex
113 development and PTC apical differentiation in the surviving mice. With the Pax8-Cre, which
114 triggers recombination in nephrogenic tubules and in nonvascular components of glomeruli
115 two days later than Wnt4-Cre (19,20), we observed normal mouse growth until postnatal (P)
116 day 14 (18). Then, body weight levelled off and all pups died at ~3-5 weeks of age, probably
117 due to kidney failure. Structural and functional studies of Vps34^{cKO} kidneys revealed
118 preserved PTC membrane polarity, but impaired apical membrane protein trafficking, thus
119 causing a general PTC dysfunction known as renal Fanconi-like syndrome, manifested by
120 polyuria and low-molecular weight proteinuria. Vps34^{cKO} also displayed impaired lysosome
121 size/positioning and blocked autophagy, thereby causing cell vacuolization. We concluded

122 that Vps34 is a crucial component of the trafficking machinery necessary for differentiated
123 PTC function and is essential for overall PTC homeostasis (18). As Pax8-Cre also triggers
124 recombination in thyrocytes, we here investigated the role of Vps34/PIK3C3 in thyroid
125 function and homeostasis.

126 ***Materials and methods***

127 *Mice*

128 Vps34$^{fl/fl}$ mice have been described (20). Pax8-Cre mice were obtained from Dr. M.
129 Busslinger (20). Vps34$^{fl/fl}$ mice were crossed with Pax8-Cre;Vps34$^{fl/+}$ mice to generate
130 conditional targeted excision of Vps34 exon 21 in the thyroid of 25% of offspring (Vps34^{cKO}).
131 Vps34$^{fl/fl}$ mice were used as control. Mice were treated according to the NIH Guide for Care
132 and Use of Laboratory Animals, and experiments were approved by the University Animal
133 Welfare Committee, Université Catholique de Louvain (2016/UCL/MD/006 and
134 2018/UCL/MD/026).

135 *Plasma, tissue collection and histology*

136 Blood was collected by eye sinus puncture at sacrifice (P14) under irreversible
137 anesthesia by xylazine 2% and ketamine 50 mg/ml (200 µl/mice i.p.). Thyroid lobes were
138 excised, fixed by immersion in neutral-buffered formaldehyde (4% F) at 4°C under stirring
139 overnight. Samples were paraffin-embedded or equilibrated overnight in 20% sucrose and
140 embedded in Tissue-Tek Optimal Cutting Medium (Sakura Finetek) for 5 µm-thick cryostat
141 sections.

142 *TSH and T4 plasma concentrations*

143 Plasma TSH concentrations were measured by a sensitive, heterologous,
144 disequilibrium double-antibody precipitation RIA as described (22). T4 concentration was
145 measured by coated-tube RIA (Siemens Medical Solution Diagnostics, Los Angeles, CA).

146 *Immunofluorescence*

147 Immunofluorescence was performed on 5 µm-thick frozen sections or on 6 µm-thick
148 paraffin sections (18). Antigen retrieval was promoted in citrate buffer, pH 6.0, at 98°C for 20
149 min using a Lab Vision Pretreatment Module™ (Thermo Scientific). After permeabilization with
150 PBS/0.3% Triton-X100 for 5 min, non-specific sites were blocked by 1-h incubation in PBS/0.3%
151 Triton-X100 with 10% bovine serum albumin (BSA) and 3% milk, followed by primary
152 antibodies (described in Supplementary Table I) in blocking buffer at 4°C overnight. After
153 extensive washing, sections were incubated with the appropriate AlexaFluor-secondary
154 antibodies in 10% BSA/0.3% Triton-X100 at room temperature for 1 h, extensively washed,
155 mounted with Faramount Aqueous Mounting Medium (Dako) and imaged on a spinning disk
156 confocal microscope using a Plan Apochromat 100x/1.4 Oil DIC objective (Cell Observer
157 Spinning Disk; Zeiss). For whole thyroid section recording, images were acquired using Zeiss
158 Mirax Midi slide scanner, stitched and analyzed using Pannoramic Viewer software.

159 *RT-qPCR*

160 Total RNA was extracted from thyroid lobes using TRIzol Reagent (Thermo Scientific),
161 as described (23). Aliquots of 500 ng RNA were reverse-transcribed by M-MLV reverse
162 transcriptase (Invitrogen) with random hexamers, as described (21). Primer sequences used
163 are described in Supplementary Table II. Real-time qPCR was performed as described (24), in
164 presence of 250 nM of specific primers with Kappa SYBR Fast qPCR Master Mix (Kapa
165 Biosystems) on a CFX96 touch real-time PCR Detection System (Bio-Rad). Data were analyzed

166 using the ΔΔCT method, using the geometric mean of *β-Actin* and *Rpl27* as reference genes
167 (25).

168 *^{125}I uptake and organification*

169 At postnatal day 8 (P8), mothers and litters were fed with an iodine-free diet for 24 h.
170 At P9, pups were injected intraperitoneally with 1 µCi ^{125}I (Perkin Elmer) and left for another
171 24 h before sacrifice and thyroid dissection. Both lobes were collected in 2 mM methimazole
172 (Sigma) and homogenized with a glass Potter. Total thyroid ^{125}I was measured with an
173 automatic gamma counter "Wizard^{2}" (Perkin Elmer) before protein precipitation using 10%
174 trichloroacetic acid (TCA; Merck). After a single wash in TCA, radioactivity was measured in
175 the protein pellet. Pourcentage of protein-bound iodide was calculated using the ratio of
176 precipitated cpm/total thyroid cpm (26).

177 *Statistical analysis*

178 All statistical analyses were determined by Prism software (GraphPad Software, La
179 Jolla, California, USA). RT-qPCR values were obtained by the ΔΔCT method and are expressed
180 as boxplots with median, 25th and 75th percentiles, and min-max whiskers. Each graph
181 represents the results form a minimum of 8 independent thyroid lobes from at least 3
182 different litters. Nonparametric statistical tests were used: Mann-Whitney for single
183 comparisons and Kruskal-Wallis followed by Dunn's post-test for more conditions. Differences
184 were considered statistically significant when $p<0.05$ (*); ** stands for $p<0.01$; *** for $p<0.001$.

185 ***Results***

186 *Genetic construction and assessment of Vps34 inactivation*

187 Global Vps34 inactivation is lethal at embryonic stage (E8.5) (27). To study the role of
188 Vps34 *in vivo,* we used a genetic approach to conditionally delete the loxP-flanked exon 21 of
189 the Vps34 gene, which encodes a critical sequence of the lipid kinase domain of Vps34 (21).
190 Tthis approach was designed to allow for the expression of a minimally truncated,
191 catalytically-inactive Vps34 protein. However, upon conditional expression in megakaryocytes,
192 the level of this truncated Vps34 and its obligatory partner, Vps15, were found to be
193 decreased by 80-90% in the megakaryocyte lineage (thrombocytes), indicating instability of
194 this truncated Vps34 protein (28). We will thus hereafter refer to the result of this type of
195 Vps34 deletion as Vps34 absence or Vps34^{cKO}.

196 We crossed homozygous Vps34$^{fl/fl}$ mice with Pax8-Cre;Vps34$^{fl/+}$ mice, which is expected
197 to lead to a tissue-specific (thyroid and kidney) conditional excision of exon 21 from both
198 Vps34 alleles in 25% of the pups (Vps34^{cKO}). Vps34^{cKO} mice were born at the expected
199 Mendelian ratio and showed normal development until postnatal day 14 (P14), then stopped
200 growing and died at around 1 month of age (18). We thus analyzed thyroid Vps34^{cKO} at P14.
201 Of note, eye opening was usually delayed till P10.

202 We first assessed the extent of Vps34 genetic excision in the thyroid by quantification
203 of its mRNA using Vps34 exon 21-specific primers. Compared to control littermate pups, we
204 found a ~70 % reduction of exon 21-containing Vps34 mRNA in cKO thyroid extracts. In
205 comparison, we found no significant difference in the abundance of Vps34 mRNA containing
206 exon 22-24 (Fig. 1A). Assuming that Vps34 is equally expressed in all thyroid cell types
207 (expressing and non-expressing the Cre recombinase), this ~70 % decrease suggests that most
208 of the thyrocytes in cKO mice had undergone Cre-dependent recombination.

209 *Vps34^{cKO} thyroid show signs of hyperstimulation by thyroid stimulating hormone (TSH)*

210 At P14, thyroid glands from Vps34^{cKO} were almost twice heavier as compared to
211 control glands (2.06 ± 0.13 mg (n=6) *versus* 1.03 ± 0.07 mg (n=8); p= 0.0024, Mann Whitney
212 test). Histological staining with Periodic-Acid-Schiff (PAS, which in the thyroid reflects
213 expression of the thyroglobulin glycoprotein) readily revealed striking differences between
214 thyroid glands of control and Vps34^{cKO} mice (Fig. 1B). Thyroid glands of controls appeared as
215 an assemblies of round follicular sections of variable diameter, filled with colloid intensely and
216 homogenously stained by PAS. In Vps34^{cKO} thyroids, follicle shape was often irregular,
217 especially at the periphery of the gland, and PAS staining was weaker or absent, indicating
218 empty lumina. Papillary projections were frequently seen in those empty lumina (Fig. 1B,
219 enlarged box). By confocal immunofluorescence microscopy, the epithelial marker, E-cadherin,
220 confirmed heterogeneity of Vps34^{cKO} follicles and revealed thicker thyrocytes. DAPI labelling
221 revealed the presence of several nuclei in a significant fraction of lumina (Fig. 1C). As these
222 histological features (follicle remodelling with thicker thyrocytes, papillary projections, and
223 colloid consumption up to exhaustion) are reminiscent to those caused by strong stimulation
224 of the thyroid gland by TSH, they suggested strong TSH stimulation of Vps34^{cKO} thyroid.

225 *Vps34^{cKO} display defective thyroglobulin iodination and proteolysis*

226 To further analyse the significance of the lack of PAS staining in a fraction of Vps34^{cKO}
227 follicles, we assessed thyroglobulin protein expression and its associated T_4 hormonogenic
228 peptide by immunofluorescence on adjacent sections. WT sections showed a perfectly
229 overlapping distribution pattern of thyroglobulin and T_4, homogeneously filling round colloidal
230 spaces (Fig. 2A). In Vps34^{cKO}, thyroglobulin labelling was much more heterogeneous and less
231 intense throughout the tissue. Remarkably, antibodies recognizing the T_4 hormonogenic
232 peptide often failed to label colloidal spaces even when containing Tg in the adjacent section

233 (Fig. 2A). Quantification revealed that only a quarter (25.2 ± 11.9 %) of the follicles were
234 labeled for T_4. These observations indicated that Vps34 ablation caused altered epithelial
235 organization, defective Tg production and/or excessive Tg consumption, as well as defective
236 thyroglobulin iodination. This further suggested that Vps34^{cKO} mice suffered from impaired T_4
237 hormone biogenesis, thus would suffer from hypothyroidism. This observation, compatible
238 with the growth retardation observed after P15, could be explained by mislocalization of one
239 or several basolateral and/or apical actors involved in thyroid hormone synthesis, as reported
240 in Vps34^{cKO} kidney proximal tubular cells (18). Of specific interest, whereas Tg signal was
241 restricted to the follicle lumen in control thyroid, Tg dots were also seen within Vps34^{cKO}
242 thyrocytes. This indicates that colloidal Tg was endocytosed by thyrocytes, but that trafficking
243 to or Tg proteolysis within the lysosomes was impaired, thus suggesting defective lysosomal
244 release of T_3/T_4, if/when hormonogenic peptides were still formed on Tg (Fig. 2B, b-d).

245 *Vps34^{cKO} causes severe non-compensated hypothyroidism*

246 To directly test the hypothesis that Vps34^{cKO} impairs thyroid hormone production,
247 plasma was collected at P14 and analyzed for T_4 and TSH levels. In control pups at that age,
248 values were 6.4 ± 1.5 μg/dL for T_4, and 75 ± 110 mU/L for TSH (Fig. 3). In Vps34^{cKO} mice, we
249 found extremely low T_4 values, often near detection level (<0.25 ± 1.5 μg/dL) and very high
250 plasma levels of TSH (19,300 ± 10,500 mU/L) (Fig. 3). These data indicate severe, non-
251 compensated hypothyroidism.

252 *Vps34 cKO display reduced iodine organification*

253 The absence of T_4-bearing Tg in Tg-containing follicles (Fig. 2A) and the undetectable
254 T_4 plasmatic levels in Vps34^{cKO} mice (Fig. 3) might be caused by defective basolateral iodine
255 uptake, apical transport and/or apical organification. Due to lack or very poor specificity of

256 antibodies directed against the proteins involved in these processes, we first measured their
257 mRNA expression levels in total thyroids at P14 (Fig. 4). We observed no change in expression
258 of *Nis*, *Tpo* and *Duox2,* a significant increase in *Tshr expression*, and a significant decrease of
259 *Duoxa2* mRNA level. At this stage, we cannot conclude if *Duoxa2* downregulation is a
260 contributing cause for the observed hypothyroidism of Vps34^{cKO}.

261 To further test whether basolateral NIS and apical TPO, DUOX and DUOXA were all
262 correctly localized, we functionally assayed their combined activity by injection of ^{125}I in pups
263 at P9, followed by a 24-h iodine deprivation and collection of thyroid lobes at P10.
264 Radioactivity was measured before and after protein precipitation by TCA (Fig. 5). ^{125}I uptake
265 was not statistically different in Vps34^{cKO} and the three control genotypes (Fig. 5A), suggesting
266 normal NIS function and thus basolateral localization. In marked contrast, only 8% of thyroid
267 ^{125}I was bound to proteins in Vps34^{cKO} compared to approximately 55% in control genotypes
268 at this stage (Fig. 5B). This indicates a major effect of Vps34 on one or several apical proteins
269 involved in iodine organification.

270 *Evaluation of lysosomal function and autophagy in Vps34^{cKO} thyroid*

271 Vps34 is involved in endocytic trafficking and autophagy. cKO of Vps34 in postnatal
272 kidney glomeruli podocytes has been reported to cause a strong increase of the overall
273 immunofluorescence signal for the lysosomal membrane marker LAMP-1, indicating
274 promotion of lysosome biogenesis (29,30). We further reported that absence of Vps34 in
275 kidney PTCs causes an increase in the actual size of lysosomes, that were sometimes enlarged,
276 and mislocalized toward the basal pole of the cell (18). Given that lysosomal proteases in
277 thyrocytes are important to excise hormonogenic peptides to release free T_3 and T_4, we
278 investigated LAMP-1-labeled structures in Vps34^{cKO} thyrocytes as a proxy for lysosomal

279 function. In our conditions, immunofluorescence on control thyroid sections only produced a
280 weak LAMP-1 signal in the E-cadherin-positive epithelial thyrocytes (Fig. 6). On the contrary,
281 a strong and widespread LAMP-1 signal was observed in all Vps34^{cKO} thyrocytes. As shown in
282 the enlarged box of Fig. 6, LAMP-1 positive late endosomes/lysosomes were enlarged and
283 sometimes vacuolated in Vps34^{cKO} thyrocytes as compared to control. This is reminiscent of
284 thyroid of cystinotic (*Ctns*$^{-/-}$) mice in which thyroid hormone production is also impaired (31).
285 The absence of Vps34 in kidney also causes a block of macroautophagy. We therefore
286 assessed the expression of p62 (also called sequestosome-1, or SQSTM1), a polyubiquitin-
287 binding protein that interacts with LC3 II (microtubule associated protein 1 light chain) on the
288 autophagosome membrane and is normally continuously degraded by the autophagy process
289 (32). Since p62 accumulates when completion of autophagy is inhibited, p62 can be used as a
290 marker to study autophagy flux (31). As shown in Fig. 7, no signal for p62 was detected in
291 control thyroid section, indicating normal autophagic flux. Conversely, Vps34^{cKO} thyrocytes
292 showed multiple p62 aggregates, indicating impaired autophagic flux, consistent with
293 defective trafficking to lysosomes. Further studies are necessary to determine if Vps34^{cKO}
294 causes abortive autophagy in thyrocytes as previously shown in kidney PTCs (18).

295 *Vps34^{cKO} follicles display luminal cells of unknown nature*

296 Surprisingly, while cells trapped in follicular lumen also showed a strong LAMP-1 signal
297 (Fig. 6), they were negative for for E-cadherin or TTF-1 expression, a permanently expressed
298 thyrocyte-specific transcription factor (Suppl Fig. 1A), indicating that these cells were not
299 derived from the thyrocyte lineage. In addition, lineage-tracing experiments on Pax8-Cre;
300 Vps34$^{fl/fl}$;ROSA-STOP-YFP pups at P14 revealed YFP positive signal only in follicle-delineating
301 thyrocytes and not in these luminal cells (Suppl Fig. 1B). Thus, luminal cells had never

302 expressed Pax8 and were thus not derived from thyrocyte progenitors. Although infiltration
303 by macrophages was an attractive alternative, we failed to label these cells for the
304 conventional macrophage marker, F4/80 (Suppl Fig. 1C). At this stage, we cannot conclude
305 about the origin of the cells trapped in follicular lumen of Vps34^{cKO} mice.

306 Further characterization of luminal cell turn-over, using immunofluorescence for
307 markers of proliferation (Ki67) and apoptosis (activated caspase 3), showed many proliferative
308 events and few apoptotic bodies (Suppl Fig. 1D). However, since proliferating cells are labeled
309 for Ki67 during most of the cell division time whereas apoptotic bodies are generally very
310 short-lived, it is not possible to assess the respective importance of proliferation and apoptosis
311 in this population. Of note, there was no appreciable change of proliferation and apoptotic
312 markers in the cKO thyrocytes themselves at P14, indicating that cell homeostasis was not
313 severely perturbed despite Vps34 absence at this stage.

314 ***Discussion***

315 In this study we report that deleting Vps34 in thyrocytes by Pax8-Cre-driven
316 recombination causes several defects in the thyroid: (i) doubling of thyroid weight and
317 perturbed thyroid parenchyma organization, with reduced PAS^{+} colloidal spaces; (ii) strong
318 decrease of ^{125}I organification, at comparable ^{125}I uptake, and of T_4 formation on thyroglobulin
319 (detected by immunofluorescence as early as P3); (iii) severe hypothyroidism with collapsed
320 plasma T_4 levels and very high TSH (documented at P14); (iv) delayed "eye opening" and
321 impaired postnatal growth after two weeks. All these features phenocopy the impact of
322 *Duoxa2* KO (34).

323 DUOXA2 is a chaperone protein required for the correct localization of DUOX2 at the
324 apical pole of thyrocyte, where the complex (DUOX2/DUOXA2) produces hydrogen peroxide.

325 In the absence of DUOXA2, hydrogen peroxide is not produced and subsequent
326 thyroperoxidase-mediated oxidation of iodide into reactive compounds and thyroglobulin
327 iodination are abolished (34). The similarity of the severity of hypothyroidism in Vps34^{cKO} and
328 *Duoxa2* KO mice prompted us pay a closer look at DUOXA2 in Vps34^{cKO}. We found that the
329 expression of *Duoxa2* started decreasing after P3, reaching two-fold lower values at P14. It is
330 interesting to note that expression of *Duox2* and *Duoxa2* mRNAs was quantitatively different,
331 despite of the fact that they share the same promoter (35). Whether decreased *Duoxa2* mRNA
332 expression is reflected by equivalent two-fold decrease of DUOX2/DUOXA2 complex at the
333 apical pole is unknown. However, it is very unlikely that a two-fold decrease would by itself so
334 severely impact on thyroglobulin iodination, since heterozygous mice for *Duoxa2* deletion
335 have virtually no phenotype. Instead, based on the known functions of Vps34 in kidney PTCs,
336 where its inactivation causes lack of apical localization of endocytic receptors (megalin,
337 cubilin) and solute transporters (NaPi-IIa, SGLT-2)(18), it would be extremely interesting to
338 localize DUOXA2 on thyroid sections, and assess apical addressing in Vps34^{cKO} thyrocytes, but
339 unfortunately no reliable antibodies are currently available. Nevertheless, ^{125}I uptake and
340 processing experiments support the hypothesis of defective apical localization of one or
341 several actors involved in thyroid hormonogenesis. While similar ^{125}I uptake in the thyroid of
342 control and Vps34^{cKO} at P10 suggests normal localization and function of the sodium-iodine
343 symporter, NIS, and/or the alternative transporter SLC26A7 (3), the major decrease of its
344 protein-bound fraction in Vps34^{cKO} are best explained by defective apical iodine transport or
345 organification.

346 Characteristic histopathological alterations combined with the very high plasma TSH
347 levels and two-fold increased *Tshr* expression in Vps34^{cKO} thyroid suggest that thyrocytes are
348 in a hyperstimulated state. However, the expression of the most sensitive target gene of the

349 TSH signaling pathway, *Nis*, was surprisingly not changed leading to the hypothesis of TSHR
350 mistrafficking into intracellular vesicles. Recent work in *Drosophila* revealed that Vps34
351 inactivation or pharmacological inhibition using the small molecule inhibitor SAR405, caused
352 alteration of cell polarity and disruption of epithelial architecture by relieving LKB1 inhibition
353 and triggering JNK activation (13). A role of Vps34 in epithelial organization and polarity was
354 also observed in 3D cultures of Caco-2 cells (13). It would be interesting to analyze the
355 activation states of LKB1 and JNK in Vps34^{cKO} thyroid, and, if modified, to cross Vps34^{cKO} with
356 LKB1 floxed alleles.

357 Our work also evidenced increased abundance and size of LAMP-1 positive late
358 endosomes/lysososmes in Vps34^{cKO} thyrocytes, with accumulation of Tg and the autophagic
359 marker, p62, indicative of a defective lysosomal trafficking and/or function. In addition to
360 impaired Tg iodination, defective thyroid hormone release might thus also result from
361 impaired endocytic transport of iodoTg to lysosomes or proteolytic excision of T_3/T_4 therein.
362 Several studies have reported a role for Vps34 for endocytic trafficking to lysosomes (12, 36,
363 37) and activation of lysosomal proteases (14). In our study on Vps34^{cKO} kidney PTCs, we also
364 observed enlargement of lysosomes and their filling by undigested material, labelled for a
365 variety of antigens (18). In Vps34^{cKO} thyrocytes, we also observed increased abundance and
366 size of LAMP-1-positive compartments. Based on these and previous findings showing that
367 Vps34 deletion leads to late endosome/lysosome enlargement and defective lysosomal
368 function (38), we assume a defective proteolytic excision of T_3/T_4 from iodoTg, analogous to
369 what we reported in cystinotic *Ctns*$^{-/-}$ mice (31). Lysosomal enlargement due to defective
370 degradation causes translocation of the transcription factor EB (TFEB), normally sequestered
371 in the cytosol, to the nucleus where it promotes the coordinate expression of genes involved

372 in lysosome biogenesis and autophagic pathways (39). TFEB translocation would readily
373 account for increased LAMP-1 signal.

374 It has recently become clear that Vps34 may act on lysosome positioning, which is
375 crucial to autophagosome formation (37,40). Similar to the kidney PTC defect, we observed
376 an increased p62 signal in Vps34^{cKO} thyroids at P14. Accumulation of p62 in Vps34^{cKO} indicates
377 a block in the autophagy process. It would be interesting to further analyse the routes to the
378 lysosomes, by analysing the activation state of Rab7, the lipidation of LC3II, and the expression
379 of LAMP2A, a marker for chaperone-mediated autophagy at lysosomes.

380 A final observation deserving discussion is the occurrence of luminal living cells.
381 Defective endocytic and autophagic routes to the lysosomes could impact thyrocyte
382 homeostasis, thus causing cellular stress. Cellular stress, induced by defective autophagosome
383 and lysosomal function, or by activation of stress kinase such as JNK, could explain shedding
384 of thyrocytes cells into the colloidal space. However, the cells that we found in the lumens of
385 Vps34^{cKO} thyroids were negative for E-cadherin and the thyrocyte-specific transcription factor,
386 TTF-1. Furthermore, using lineage tracing experiments, we demonstrated that these luminal
387 cells had never expressed Pax8 and thus did not derive from thyrocytes. Alternatively, we
388 examined whether luminal cells could derive from mesenchymal cells, in particular infiltrating
389 macrophages. We know that these cells have high LAMP-1 signal, are proliferating, and must
390 have invasive properties to cross the follicular monolayer and its surrounding basal lamina,
391 before reaching the colloid. However, luminal cells were not labelled for the conventional
392 macrophage marker, F4/80, admittedly not a universal macrophage identifier. The origin of
393 infiltrating cells and the cause of high LAMP1 are thus still unknown.

394 ***Acknowledgements***

395 This work was supported by grants from the Fonds pour la Recherche Scientifique (F.R.S-FNRS,
396 # J.0076.18, Belgium), Université catholique de Louvain (Actions de Recherche concertées to
397 CEP, ARC 15/20-065), and Fondation Roi Baudouin. SR and X-HL were supported by a grant
398 DK15070 from the National Institutes of Health, USA. Work in the laboratory of BV was
399 supported by grants from the MRC (G0700755) and BBSRC (BB/I007806/1; BB/M013278/1).
400 The core facility for Imaging Cells and Tissues was also financed by National Lottery, Région
401 bruxelloise, Région wallonne, Université catholique de Louvain and de Duve Institute. The
402 authors thank Abdelkadder El Kaddouri and Claude Massart for technical help. GG held a
403 fellowship from the Fonds pour la formation à la Recherche dans l'Industrie et l'Agriculture
404 (FRIA, Belgium), TW was postdoctoral researcher supported by UCLouvain, VJ is supported by
405 the Cystinosis Research Foundation, CS is a UCLouvain teaching assistant, HGC was a
406 postdoctoral researcher and CEP is a Senior Research Associate at F.R.S-FNRS.

407 **Authors disclosures and contributions**

408 BV is a consultant for Karus Therapeutics (Oxford, UK), iOnctura (Geneva, Switzerland) and
409 Venthera (Palo Alto, US) and has received speaker fees from Gilead. The other authors have
410 no competing financial interest. GG and TSW performed the morphological and molecular
411 studies and analyzed the data. OD, VJ, CS and AS participated in data collection and analysis.
412 HGC was involved in supervision of GG. BB and BV provided the Vps34 mice, XHL and SR
413 assayed T4 and TSH levels, and CM provided expertise with ^{125}I experiments. PJC and CEP
414 conceived, designed and supervised the project, and wrote the manuscript. All authors
415 have approved the final version of the manuscript.

416 **Name and address of corresponding author**

417 Prof. Christophe E. Pierreux

418 Cell Biology Unit

419 de Duve Institute and Université Catholique de Louvain

420 75, Avenue Hippocrate

421 B-1200 Brussels

422 Belgium

423 Email : christophe.pierreux@uclouvain.be

424 ***References***

425 1. Colin IM, Denef JF, Lengele B, Many MC, Gerard AC 2013 Recent insights into the cell biology

426 of thyroid angiofollicular units. Endocr Rev 34:209-238.

427 2. Carvalho DP, Dupuy C 2017 Thyroid hormone biosynthesis and release. Mol Cell Endocrinol

428 458:6-15.

429 3. Cangul H, Liao X-H, Schoenmakers E, Kero J, Barone S, Srichomkwun P, Iwayama H, Serra

430 EG, Saglam H, Eren E, Tarim O, Nicholas AK, Zvetkova I, Anderson CA, Karet Frankl FE,

431 Boelaert K, Ojaniemi M, Jääskeläinen J, Patyra K, Löf C, Williams ED, UK10K Consortium,

432 Soleimani M, Barrett T, Maher ER, Chatterjee VK, Refetoff S, Schoenmakers N 2018

433 Homozygous loss-of-function mutations in SLC26A7 cause goitrous congenital

434 hypothyroidism. J Clin Ivest Insight 3:e99631.

435 4. Koumarianou P, Gomez-Lopez G, Santisteban P 2017 Pax8 controls thyroid follicular polarity

436 through cadherin-16. J Cell Sci 130:219-231.

437 5. Shivas JM, Morrison HA, Bilder D, Skop AR 2010 Polarity and endocytosis: reciprocal

438 regulation. Trends Cell Biol 20:445-452.

439 6. Rodriguez-Boulan E, Macara IG 2014 Organization and execution of the epithelial polarity
440 programme. Nat Rev Mol Cell Biol 15:225-242.
441 7. Morrison HA, Dionne H, Rusten TE, Brech A, Fisher WW, Pfeiffer BD, Celniker SE, Stenmark
442 H, Bilder D 2008 Regulation of early endosomal entry by the Drosophila tumor
443 suppressors Rabenosyn and Vps45. Mol Biol Cell 19:4167-4176.
444 8. Lindmo K, Stenmark H 2006 Regulation of membrane traffic by phosphoinositide 3-kinases.
445 J Cell Sci 119:605-614.
446 9. Juhasz G, Hill JH, Yan Y,Sass M, Baehrecke EH, Backer JM, Neufeld TP 2008 The class III PI(3)K
447 Vps34 promotes autophagy and endocytosis but not TOR signaling in Drosophila. J Cell
448 Biol 181:655-666.
449 10. Backer JM 2008 The regulation and function of Class III PI3Ks: novel roles for Vps34.
450 Biochem J 410:1-17.
451 11. Jaber N, Zong WX 2013 Class III PI3K Vps34: essential roles in autophagy, endocytosis, and
452 heart and liver function. Ann NY Acad Sci 1280:48-51.
453 12. Bechtel W, Helmstädter M, Balica J, Hartleben B, Kiefer B, Hrnjic F, Schell C, Kretz O, Liu S,
454 Geist F, Kerjaschki D, Walz G, Huber TB 2013 Vps34 deficiency reveals the importance
455 of endocytosis for podocyte homeostasis. J Am Soc Nephrol 24:727-743.
456 13. O'Farrell F, Lobert VH, Sneeggen M, Jain A, Katheder NS, Wenzel EM, Schultz SW, Tan KW,
457 Brech A, Stenmark H, Rusten TE 2017 Class III phosphatidylinositol-3-OH kinase
458 controls epithelial integrity through endosomal LKB1 regulation. Nat Cell Biol 19:1412-
459 1423.
460 14. Ronan B, Flamand O, Vescovi L, Dureuil C, Durand L, Fassy F, Bachelot M-F, Lamberton A,
461 Mathieu M, Bertrand T, Marquette J-P, El-Ahmad Y, Filoche-Romme B, Schio L, Garcia-

462 Echeverria C, Goulaouic H, Pasquier B 2014 A highly potent and selective Vps34
463 inhibitor alters vesicle trafficking and autophagy. Nat Chem Biol 10:1013-1019.
464 15. Nascimbeni AC, Codogno P, Morel E 2017 Phosphatidylinositol-3-phosphate in the
465 regulation of autophagy membrane dynamics. FEBS J 284:1267-1278.
466 16. Dupont N, Nascimbeni AC, Morel E, Codogno P 2017 Molecular Mechanisms of
467 Noncanonical Autophagy. Intl Rev Cell Mol Biol 328:1-23.
468 17. Carpentier S, N'Kuli F, Grieco G, Van Der Smissen P, Janssens V, Emonard H, Bilanges B,
469 Vanhaesebroeck B, Gaide Chevronnay HP, Pierreux CE, Tyteca D, Courtoy PJ 2013
470 ClassIII phosphoinositide 3-kinase/VPS34 and dynamin are critical for apical endocytic
471 recycling. Traffic 14:933-948.
472 18. Grieco G, Janssens V, Gaide Chevronnay HP, N'Kuli F, Van Der Smissen P, Wang TS, Shan J,
473 Vainio S, Bilanges B, Jouret F, Vanhaesebroeck B, Pierreux CE, Courtoy PJ 2018
474 Suppression of Vps34 PI 3-kinase activity in kidney proximal tubules abrogates apical
475 trafficking and causes a Fanconi syndrome. Sci Rep 8:14133.
476 19. Shan J, Jokela T, Skovorodkin I, Vainio S 2010 Mapping of the fate of cell lineages generated
477 from cells that express the Wnt4 gene by time-lapse during kidney development.
478 Differentiation 79:57-64.
479 20. Bouchard M, Souabni A, Busslinger M 2004 Tissue-specific expression of cre recombinase
480 from the Pax8 locus. Genesis 38:105-109.
481 21. Valet C, Levade M, Chicanne G, Bilanges B, Cabou C, Viaud J, Gratacap MP, Gaits-Iacovoni
482 F, Vanhaesebroeck B, Payrastre B, Severin S 2017 A dual role for the class III PI3K,
483 Vps34, in platelet production and thrombus growth. Blood 130:2032-2042.
484 22. Pohlenz J, Maqueem A, Cua K, Weiss RE, Van Sande J, Refetoff S 1999 Improved
485 radioimmunoassay for measurement of mouse thyrotropin in serum: strain

486 differences in thyrotropin concentration and thyrotroph sensitivity to thyroid
487 hormone. Thyroid 9:1265-1271.
488 23. Delmarcelle AS, Villacorte M, Hick AC, Pierreux CE 2014 An ex vivo culture system to study
489 thyroid development. J Vis Exp 6:88.
490 24. Hick AC, Delmarcelle AS, Bouquet M, Klotz S, Copetti T, Forez C, Van Der Smissen P,
491 Sonveaux P, Collet JF, Feron O, Courtoy PJ, Pierreux CE 2013 Reciprocal
492 epithelial:endothelial paracrine interactions during thyroid development govern
493 follicular organization and C-cells differentiation. Dev Biol 381:227-240.
494 25. Dupasquier S, Delmarcelle AS, Marbaix E, Cosyns JP, Courtoy PJ, Pierreux CE 2014
495 Validation of housekeeping gene and impact on normalized gene expression in clear
496 cell renal cell carcinoma: critical reassessment of YBX3/ZONAB/CSDA expression. BMC
497 Mol Biol 15:9.
498 26. Massart C, Hoste C, Virion A, Ruf J, Dumont JE, Van Sande J 2011 Cell biology of H2O2
499 generation in the thyroid: investigation of the control of dual oxidases (DUOX) activity
500 in intact ex vivo thyroid tissue and cell lines. Mol Cell Endocrinol 343:32-44.
501 27. Zhou X, Takatoh J, Wang F 2011 The mammalian class 3 PI3K (PIK3C3) is required for early
502 embryogenesis and cell proliferation. PloS one 6:e16358.
503 28. Bilanges B, Alliouchene S, Pearce W, Morelli D, Szabadkai G, Chung YL, Chicanne G, Valet
504 C, Hill JM, Voshol PJ, Colinson L, Peddie C, Ali K, Ghazaly E, Rajeeve V, Trichas G, Srinivas
505 S, Chaussade C, Salomon RS, Backer JM, Scudamore CL, Whitehead MA, Keaney EP,
506 Murphy LO, Semple RK, Payrastre B, Tooze SA, Vanhaesebroeck B 2017 Vps34 PI 3-
507 kinase inactivation enhances insulin sensitivity through reprogramming of
508 mitochondrial metabolism. Nat Commun 8:1804.

509 29. Chen J, Chen MX, Fogo AB, Harris RC, Chen JK 2013 mVps34 deletion in podocytes causes
510 glomerulosclerosis by disrupting intracellular vesicle trafficking. J Am Soc Nephrol.
511 24:198-207.
512 30. Bechtel, W, Helmstädter M, Balica J, Hartleben B, Schell C, Huber TB 2013 The class III
513 phosphatidylinositol 3-kinase PIK3C3/VPS34 regulates endocytosis and
514 autophagosome-autolysosome formation in podocytes. Autophagy 9:1097-1099.
515 31. Gaide Chevronnay HP, Janssens V, Van Der Smissen P, Liao XH, Abid Y, Nevo N, Antignac C,
516 Refetoff S, Cherqui S, Pierreux CE, Courtoy PJ 2015 A mouse model suggests two
517 mechanisms for thyroid alterations in infantile cystinosis: decreased thyroglobulin
518 synthesis due to endoplasmic reticulum stress/unfolded protein response and
519 impaired lysosomal processing. Endocrinology 156:2349-2364.
520 32. Cohen-Kaplan V, Ciechanover A, Livneh I 2016 p62 at the crossroad of the ubiquitin-
521 proteasome system and autophagy. Oncotarget 7:83833-83834.
522 33. Bjorkoy G, Lamark T, Pankiv S, Overvatn A, Brech A, Johansen T 2009 Monitoring
523 autophagic degradation of p62/SQSTM1. Methods Enzymol 452:181-197.
524 34. Grasberger H, De Deken X, Mayo OB, Raad H, Weiss M, Liao XH, Refetoff S 2012 Mice
525 deficient in dual oxidase maturation factors are severely hypothyroid. Mol Endocrinol
526 26:481-492.
527 35. Christophe-Hobertus C, Christophe D 2010 Delimitation and functional characterization of
528 the bidirectional THOX-DUOXA promoter regions in thyrocytes. Mol Cell Endocrinol
529 317:161-167.
530 36. Pasquier B 2015 SAR405, a PIK3C3/Vps34 inhibitor that prevents autophagy and synergizes
531 with MTOR inhibition in tumor cells. Autophagy 11:725-726.

532 37. Hong Z, Pedersen NM, Wang L, Torgersen ML, Stenmark H, Raiborg C 2017 PtdIns3P
533 controls mTORC1 signaling through lysosomal positioning. J Cell Biol 216:4217-4233.
534 38. Jaber N, Mohd-Naim N, Wang Z, DeLeon JL, Kim S, Zhong H, Sheshadri N, Dou Z, Edinger
535 AL, Du G, Braga VM, Zong WX 2016 Vps34 regulates Rab7 and late endocytic trafficking
536 through recruitment of the GTPase-activating protein Armus. J Cell Sci 129:4424-4435.
537 39. Settembre C, De Cegli R, Mansueto G, Saha PK, Vetrini F, Visvikis O, Huynh T, Carissilo A,
538 Palmer C, Klisch TJ, Wollenberg AC, Di Bernardo D, Chan L, Irazoqui JE, Ballabio A 2013
539 TFEB controls cellular lipid metabolism through a starvation-induced autoregulatory
540 loop. Nat Cell Biol 15:647-658.
541 40. Korolchuk VI, Rubinsztein DC 2011 Regulation of autophagy by lysosomal positioning.
542 Autophagy 7:927-928.

543

544 *Supplementary Table I: Antibodies and use*

545

Antibody	Supplier	Reference	Species	Dilution	Unmasking	Embedding
E-Cadherin	BD Biosciences	610182	mouse IgG2a	1/1000	- or +	paraffin or gelatin
Thyroglobulin	DAKO	M0781	mouse IgG1	1/500	+	paraffin
T4	MyBiosource	MBS211305	mouse IgG1	1/1000	+	paraffin
LAMP-1	Hybridoma Bank	1D4B	rat (Mab)	1/100	-	paraffin or gelatin
P62	ARP	03-GP62C	guinea pig	1/400	+	paraffin or gelatin
TTF1	Agilent	M357501	mouse IgG1	1/200	+	paraffin
F4/80	Abcam	Ab6640	rat	1/200	+	paraffin
YFP	Abcam	Ab6673	goat	1/250	+	Paraffin or gelatin
Ki67	BD Biosciences	556003	mouse IgG1	1/250	+	paraffin
Act. Casp. 3	Cell signalling	9661	rabbit	1/100	+	paraffin

546

547

548

549 *Supplementary Table II: Primers*

550

gene	forward primer (5' → 3')	reverse primer (5' → 3')
Vps34 ex20-21	CACACAGTATCCAGCACAGC	TGAGACTGGACCCTATGGCA
Vps34 ex21-22	TTGGAGTTGGAGACCGGCA	TCCTTGTTCAGCTTCATCGGAG
Vps34 ex22-24	GATGGTGGAAGGGATGGGTG	CGCTCTCGTCGATCAGACTC
Cdh1	AGGGAGCTGTCTACCAAAGTG	CCAGTCTCGTTTCTGTCTTC
Nis	AGCAGGCTTAGCTGTATCCC	AGCCCCGTAGTAGAGATAGGAG
Tpo	TGCCAACAGAAGCATGGGCAAC	GCACAAAGTTCCCATTGTCCAC
Tshr	CTGCGGGGCAAAGAGTGTGC	AGGGGAGCTCTGTCAAGGCA
Tg	TGGGACGTGAAAGGGGAATGGTGC	GTGAGCTTTTGGAATGGCAGGCGA
Duox	TCCAGAAGGCGCTGAACAG	GCGACCAAAGTGGGTGATG
Duoxa2	CGTTAACATTACACTCCGAGGAACA	CAGAATGCCACCCACAGTGT
b-actin	TCCTGAGCGCAAGTACTCTGT	CTGATCCACATCTGCTGGAAG
Rpl27	GCCCTGGTGGCTGGAATTGACC	AAACTTGACCTTGGCCTCCCGC

551

552

553

554

555

Figure legends

Figure 1. Genetic and histopathological characterization. A. Extensive genetic excision of Vps34 exon 21. Compared with control (black boxes), Vps34^{cKO} thyroid (red boxes) shows ~70% reduction in exon 21 mRNA level at P14. The unchanged mRNA level spanning exons 22-24 serves as control. Boxes with median and percentiles of 10 WT and 11 cKO samples; ***, p< 0.0001 by Mann-Whitney non-parametric test. ***B. Histopathological evidence of follicle hyperactivity*.** As compared to control thyroid tissue where all follicles show lumen filling with homogenous PAS (Periodic Acid Shiff) staining, Vps34^{cKO} thyroid presents fewer, mostly centrally located, PAS-stained follicles and with weaker staining intensity, other follicles that appear empty (arrows), and still other with papillary projections into the luminal space (arrowheads and enlarged box in the inset). All these alterations are characteristic of follicle hyperactivity. ***C. Vps34^{cKO} thyrocytes are altered and follicles contains abundant non-epithelial cells***. Nuclei are labeled by Hoechst (presented in white); thyrocyte basolateral contours are labeled for E-cadherin (red); two lumen boundaries are delineated by broken lines. As compared to control thyroid follicles, Vps34^{cKO} follicular structures are frequently less organized, circumscribed by thicker thyrocytes and containing additional cells inside the lumen (yellow arrowheads). These cells are not labeled for E-cadherin (for further characterization, see Supplementary Figure 1).

***Figure 2. Evidence for defective iodide organification in Vps34^{cKO} thyroid: follicular lumina with Tg but devoid of iodinated-Tg.* A.** Semi-serial thyroid sections from control (left) and Vps34^{cKO} (right) labeled for E-cadherin (green) and thyroglobulin (red), recognized either for a proteic epitope (Tg), or a hormonogenic peptide (T4). Control follicular lumina are round and

25 uniformly labeled for both Tg and T4. In Vps34^{cKO}, follicular structures are less regular, with the
26 majority that are filled of Tg (in this field), are without T4 signal. ***B. Comparison of Tg labelling***
27 ***in control (a) and Vps34^{cKO} thyrocytes (b-d).*** In control follicles (a), Tg is essentially restricted
28 to lumen, with little or no signal inside thyrocytes. In Vps34^{cKO} (b-d), Tg is often less abundant
29 in the lumen, but readily detected within thyrocytes as collections of submicrometric dots
30 (small arrowheads) or larger spheres (large arrowhead). Of note, some luminal cells (c, broken
31 line) also contain Tg-labeled spheres, indicating active endocytosis (arrow).
32
33 ***Figure 3. Vps34^{cKO} mice display severe hypothyroidism associated with strong TSH***
34 ***production.*** As compared to control mice (black circles), T_4 blood level in Vps34^{cKO} is extremely
35 low, if not at the detection level (red circles). Conversely, TSH levels are dramatically elevated.
36 (10 WT and 9 cKO samples; ***, p = 0.0003 by Mann-Whitney non-parametric test).
37
38 ***Figure 4. Relative expression level of principal actors in thyroid hormonogenesis at P14***. Gene
39 expression analysis by RT-qPCR, presented as boxes with median and percentiles. As
40 compared to control thyroid (black boxes), expression in Vps34^{cKO} (red boxes) is preserved for
41 the epithelial marker E-cadherin (*Cdh1)*, and the thyroid-specific genes *Nis*, *Tpo*, *Tg* and *Duox2.*
42 Expression of the TSH receptor (*Tshr*) is significantly increased in Vps34^{cKO}, consistent with a
43 TSH response, while expression of *Duoxa2* is significantly decreased. Boxes with median and
44 percentiles of 10 WT and 11 cKO samples; ***, p= 0.0005 by Mann-Whitney non-parametric
45 test.
46
47 ***Figure 5. Normal uptake of iodine but major defects of organification in Vps34^{cKO} thyroids.***
48 ***A.*** Comparable ^{125}I-iodine uptake in the thyroid of the three control genotypes (black boxes)

49 and Vps34^{cKO} thyroid (red box). **B**. Compared to the three control genotypes, the percentage
50 of ^{125}I bound to protein is much reduced in Vps34^{cKO} thyroid, suggesting defective
51 organification. Boxes with median and percentiles of 10 Flox/+, 19 Flox/Flox, 10 Cre;Flox/+
52 and 10 Vps34^{cKO} (Cre;Flox/Flox) samples; ***, $p < 0.001$ by Kruskal-Wallis test with Dunn's
53 multiple comparison test.

54

55 ***Figure 6. Vps34^{cKO} thyrocytes and luminal cells display increased LAMP-1 signal (green).***
56 Thyrocytes are labeled by E-cadherin (red). As compared to control follicles which uniformly
57 show a weak signal for the lysosomal marker LAMP-1, this signal is intense in Vps34^{cKO}
58 thyrocytes and in cells present in the colloidal space (arrows). Broken lines indicate luminal
59 contours. As shown in the enlargements below, LAMP-1-labeled structures in Vps34 cKO
60 thyrocytes are enlarged compared with WT (small arrowheads) or vacuolated (large
61 arrowheads).

62

63 ***Figure 7. Vps34^{cKO} thyrocytes show strong accumulation of p62 dots outside LAMP-1.***
64 Immunolocalization of LAMP-1 (green), and p62 (red). Compared with control follicles, which
65 show a weak signal for the LAMP-1 and no signal for p62, both signals are very strong in
66 Vps34^{cKO} thyroid sections. p62 label aggregates up to 5 μm in diameter (large arrowhead in
67 the enlargement). These aggregates show no signal for LAMP-1, indicating failure to reach
68 lysosomes.

69

70 ***Suppl Fig. 1. Further characterization of luminal cells in Vps34^{cKO} thyroid.***
71 ***A. Luminal cells are not thyrocytes*.** Immunolabelling for thyrocyte transcription factor-1 (TTF-
72 1, green); nuclei are visualized with the Hoechst stain (represented in white for better

visualization). In both control and cKO thyroid, nuclei of thyrocytes circumscribing the follicular lumina are all labeled by the thyrocyte-specific transcription-factor-1, TTF-1. As indicated by the yellow arrowhead, nuclei of luminal cells show no signal for TTF-1 (only white signal representing Hoechst). ***B. Luminal cells do not derive from thyrocyte progenitors.*** Immunolabelling for E-cadherin (red) and YFP (green); nuclei are visualized with the Hoechst stain(blue). Representative images of Vps34cKO thyroid sections reveal expression of YFP only in cells surrounding the follicular lumina, i.e. in cells where Pax8-Cre has been active. Luminal cells do not derive from thyrocyte progenitors as they are negative for YFP. ***C. Luminal cells are not conventional macrophages*.** Immunolabelling for E-cadherin (red), and for the conventional macrophage marker (F4/80, green) + Hoechst (white). In control thyroid, F4/80 signal is restricted to the interstitium. In Vps34^{cKO}, luminal cells identified by Hoechst show no signal for F4/80 (yellow arrowheads). **D. Luminal cells are proliferating.** Immunolabelling for E-cadherin (red), proliferation (Ki67, shown in white) and apoptosis (activated caspase 3, green). In developing control thyroid at P14, Ki67 labels mostly round thyrocyte nuclei (arrow) and elongated interstitial nuclei (arrowhead). In Vps34^{cKO} follicles, luminal cells show evidence of proliferation (arrows) and apoptosis (arrowhead). Broken lines indicate luminal contours.

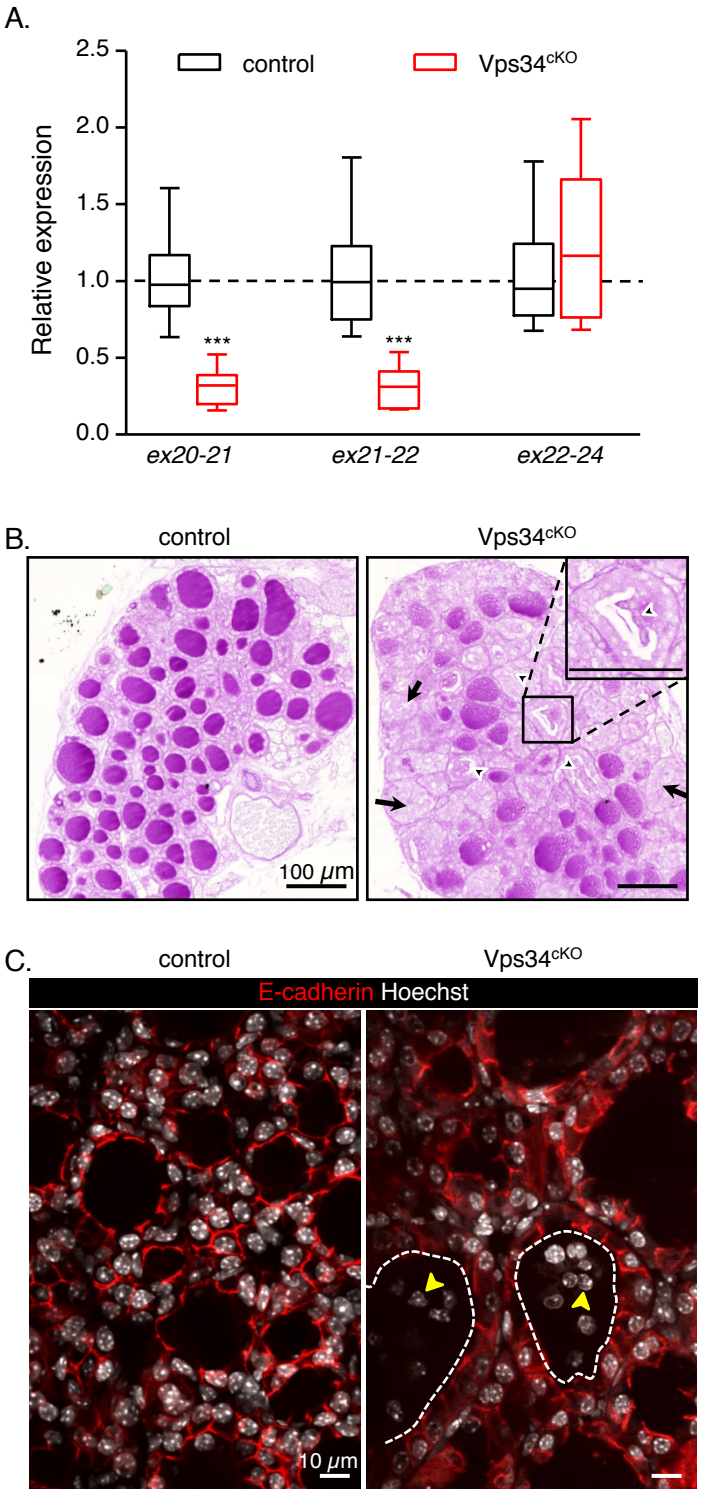
A.
control
Vps34cKO
Relative expression
2.5
2.0
1.5
1.0
0.5
0.0
***
***
ex20-21
ex21-22
ex22-24
B.
control
Vps34cKO
100 μm
C.
control
Vps34cKO
E-cadherin Hoechst
10 μm

GriecoFig1

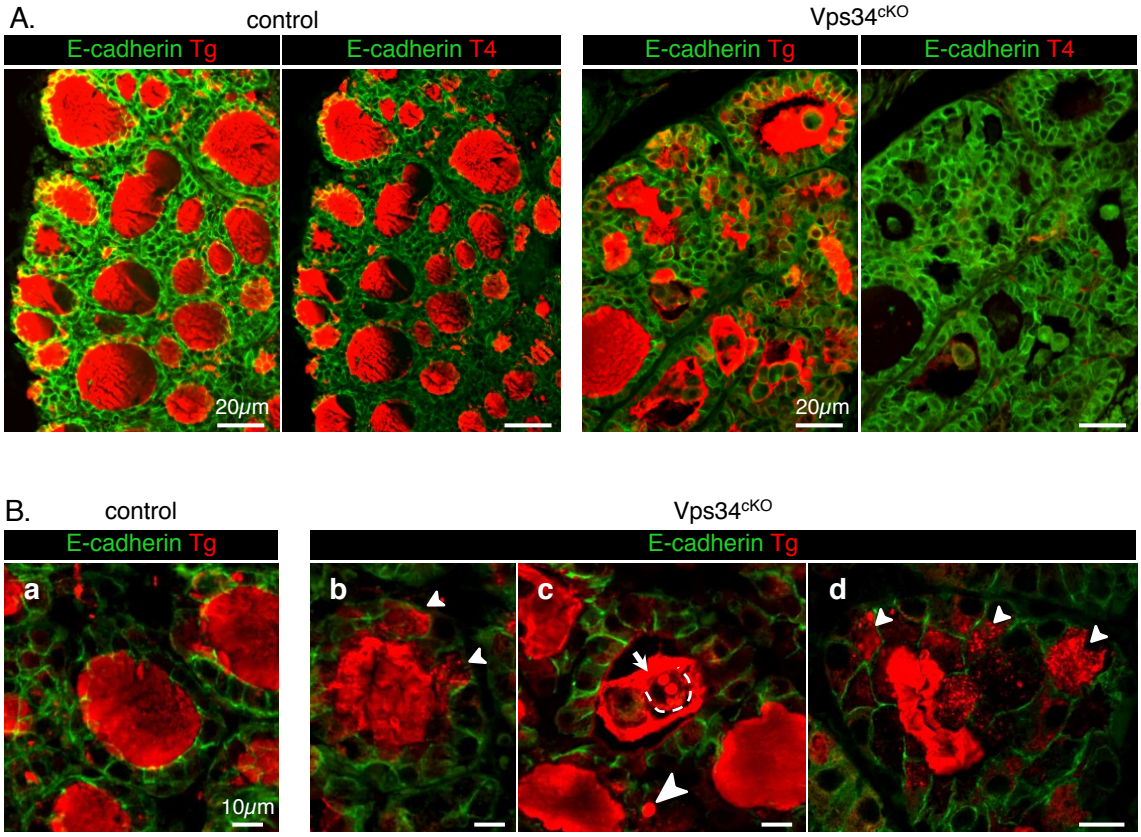
A.
control
Vps34cKO
E-cadherin Tg
E-cadherin T4
E-cadherin Tg
E-cadherin T4
20μm
20μm
B.
control
Vps34cKO
E-cadherin Tg
E-cadherin Tg
a
b
c
d
10μm

GriecoFig2

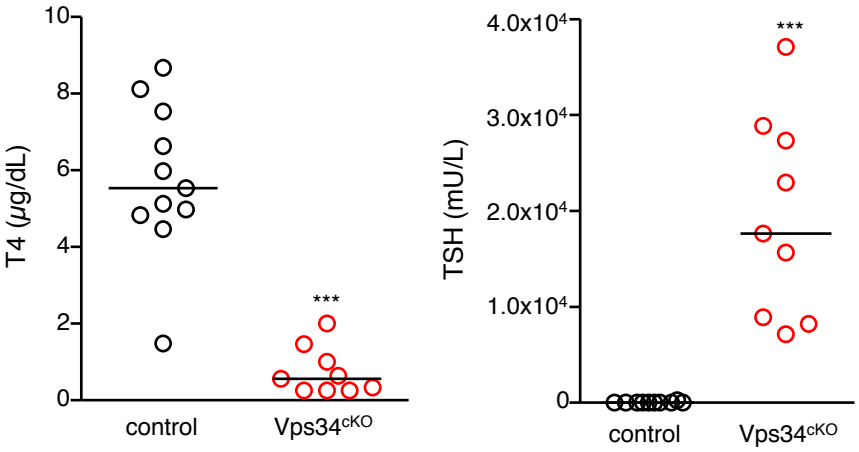
10
8
6
4
2
0
T4 (μg/dL)
***
control
Vps34cKO
4.0x10⁴
3.0x10⁴
2.0x10⁴
1.0x10⁴
0
TSH (mU/L)
***
control
Vps34cKO

GriecoFig3

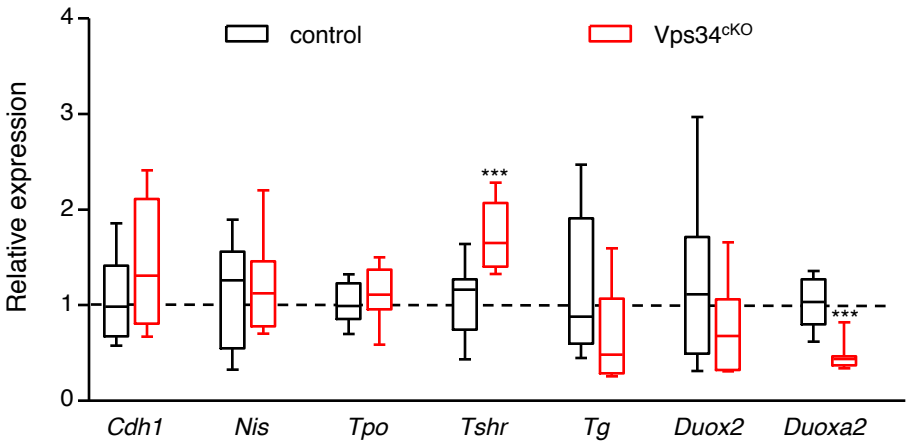
control
Vps34cKO
Relative expression
4
3
2
1
0
***
***
Cdh1
Nis
Tpo
Tshr
Tg
Duox2
Duoxa2

GriecoFig4

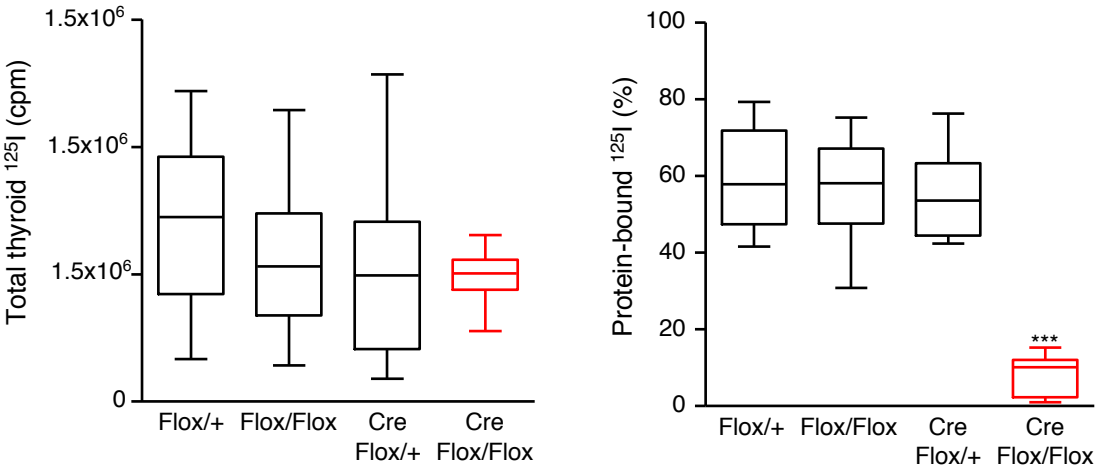
Total thyroid 125I (cpm)
1.5x10^6
1.5x10^6
1.5x10^6
0
Flox/+
Flox/Flox
Cre Flox/+
Cre Flox/Flox
Protein-bound 125I (%)
100
80
60
40
20
0
***
Flox/+
Flox/Flox
Cre Flox/+
Cre Flox/Flox

GriecoFig5

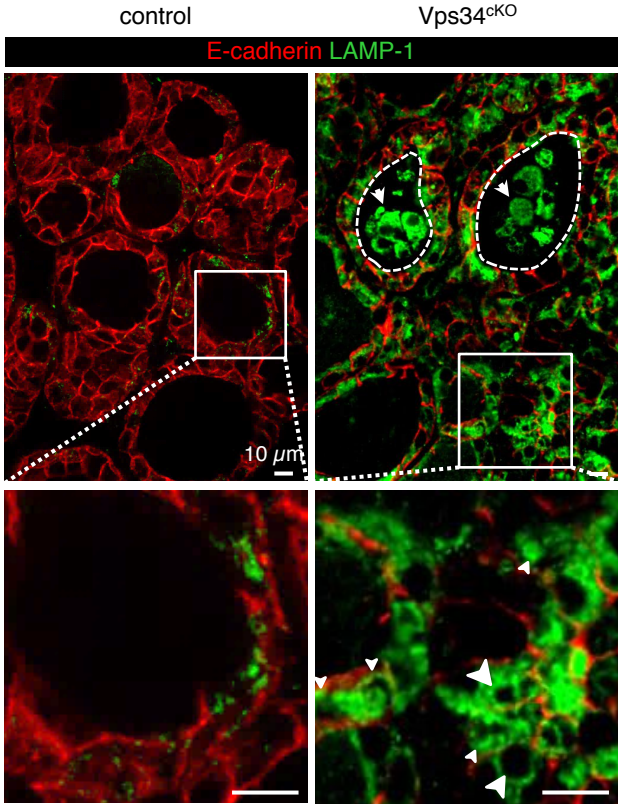

GriecoFig6

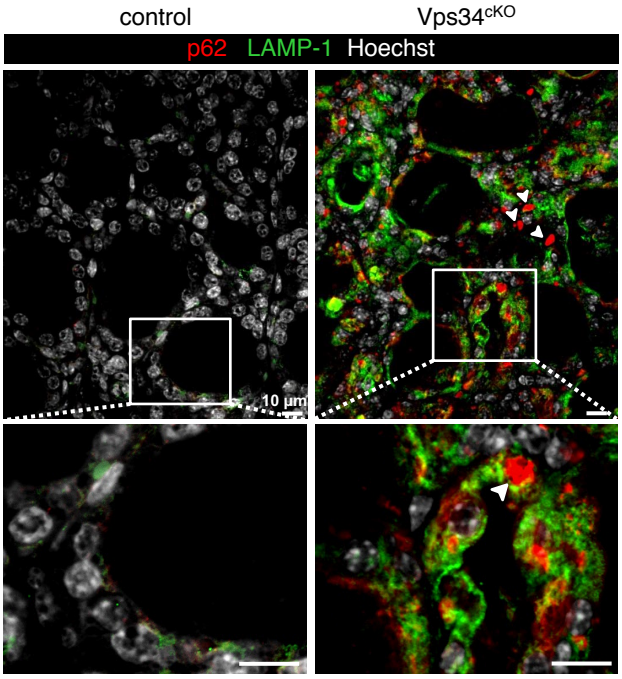

GriecoFig7